



Analysis of the photo-thermal excitation in a semiconducting medium under the purview of DPL theory involving non-local effect

Ravi Kumar · Rakhi Tiwari · Abhinav Singhal

Received: 28 August 2021 / Accepted: 18 April 2022 / Published online: 25 May 2022
© Springer Nature B.V. 2022

Abstract Non-local theory comprises a unique characteristics by analyzing the effects of all points of the body on a single point of the material. The present study enlightens the propagation of photo-thermal waves in a semiconductor by adopting the two phase lag theory of thermoelasticity in the frame of non-local effect. Normal mode analysis has been employed to obtain the exact expressions of the field quantities such as temperature, components of the displacement, carrier density, and components of the stress. Each field quantity is found to be influenced by the non-local parameter as well as phase lags. Quantitative results are determined in the time-domain by adopting a suitable technique of Laplace transform inversion which exhibit the influence of the non-locality effect on the distributions of field variables. Significant differences have been attributable to the studied fields due to the non-locality effect. Also,

computational results are compared with the corresponding results obtained by using single phase lag theory proposed by Lord and Shulman (LS model)LS model single phase lag model (LS model).

Keywords Photo thermal waves · Dual phase lag heat conduction · Normal mode analysis · Non-local effect

Abbreviations

T	Temperature
T_0	Reference temperature
u	Displacement vector
N	Carrier density
σ_{ij}	Stress components
e_{ij}	Strain components
λ, μ	Lame' constants, $\gamma = (3\lambda + 2\mu)\alpha_t$
α_t	Thermal expansion coefficient
d_n	Coefficient of electronic deformation
δ_n	Difference of deformation potential of conduction and valence band and $\delta_n = (3\lambda + 2\mu)d_n$
δ_{ij}	Kronecker delta
K	Thermal conductivity
ρ	Mass density
c_v	Specific heat at constant volume
E_g	Energy gap of the semiconductor
D_E	Carrier diffusion coefficient
τ	Photo-generated carrier lifetime
τ_T	Phase-lag due to temperature gradient

R. Kumar
Department of Mathematics, Central University of South Bihar, Fatehpur 824236, India

R. Tiwari (✉)
Department of Mathematics, Nitishwar College, A Constituent Unit of Babasaheb Bhimrao Ambedkar Bihar University, Muzaffarpur 842002, India
e-mail: rakhitiwari.rs.apm12@itbhu.ac.in

A. Singhal
Department of Computational Sciences, Delhi NCR Campus, Christ (Deemed to be University), Ghaziabad, UP 201003, India

$$\kappa = \frac{\tau_q}{\tau} \frac{\partial N_0}{\partial T}$$

Phase-lag due to heat flux vector
 N_0 : carrier concentration at a temperature
 T

1 Introduction

The theory of generalized thermoelasticity is seeking the attention of researchers and scientists for the last thirty years due to its potentiality to predict the finite speed of thermal waves which is in contrast with the concept of the classical theory of thermoelasticity. Also, this theory exhibits several applications in various fields such as physics, geophysics, chemistry, aeronautics, nuclear reactors, mineral exploration, earth quake prediction and modern engineering. The classical theory is described by Fourier's law which supports the parabolic nature of heat conduction i.e. infinite speed of thermal waves which may be applicable in particular situations such as high heat flux problems, problems with large spatial dimension, etc. but ultimately this theory is found to be incapable for realistic outcomes of several concrete problems. Biot [1] presented the detailed formulation of the classical theory of thermoelasticity based on the Fourier law of heat conduction. However, this theory gained popularity as an efficient model to study the coupling effect of the thermal and elastic fields. But, due to its parabolic nature of thermal conduction, several new concepts such as modifying consecutive equations, the concept of phase-lags, introducing new consecutive variables as well as involve non-local concepts, etc. have been executed by researchers. Later on, Lord and Shulman [2] (LS) proposed a model by inserting one relaxation time parameter in Fourier's law of heat conduction. This model predicts the hyperbolic nature of the heat conduction equation. Further, the generalization of the LS model was established by Green and Lindsay [3] (GL). Dhaliwal and Sherief [4] extended the LS theory to the problems with an anisotropic medium. After that, it was noticed that the materials involving higher values of relaxation times of heat propagation were needing a new approach apart from the LS theory and GL theory of thermoelasticity. Then, three new theories have been constructed by Green and Naghdi [5–7]. These theories are attributed as Green-Naghdi I theory of thermoelasticity (GN-I), Green-Naghdi II theory of thermoelasticity (GN-II), and Green-Naghdi III theory of

thermoelasticity (GN-III). Tiwari and Mukhopadhyay [8] studied magneto-thermoelastic problem under the purview of GN-II theory of thermoelasticity. A study of thermoelastic damping in micromechanical resonators under unified generalized thermoelasticity formulation is given by Kumar and Kumar [9].

Further, it was noticed that micro and nano engineering are of higher demand; therefore, a more generalized model was investigated by Tzou [10, 11] and Chandrasekharaiah [12, 13]. Tzou [10] inserted two phase lag parameters: one corresponding to the heat flux vector and the other for the temperature gradient in the Fourier law of heat conduction equation and this law achieved fame as a dual phase lag heat conduction model. Dual phase lag theory specifies the interactions among electrons and phonons that occur at a microscopic level and act as the delaying sources. Many problems are solved by the researchers with the concept of phase lags [14–17]. El-Karamany and Ezzat [18] published an article on the dual-phase-lag thermoelasticity theory. Magaña and Quintanilla [19] studied existence and uniqueness of phase-lag thermoelasticity. Rezazadeh et al. [20] gave an analysis of bias DC voltage effect on thermoelastic damping ratio in short nano-beam resonators based on non-local elasticity theory and dual-phase-lagging heat conduction model.

The semiconductor elastic materials as silicon have multifold applications in the prospect of modern physics like transducers, resonators, sensors, filters, etc. Photothermal technologies are extensively used in studying the vibrations and microelectronic structures due to its unique properties such as non-contact and non-destructive. Photothermal theory and semiconductor materials have a very strong bonding due to their huge importance in nano-materials technology such as solar cells. A mechanical change and thermal load are observed when a semiconductor elastic medium is excited by photothermal.

The excitation of short elastic pulses by photothermal are useful in several different branches of science. These studies are helpful for the monitoring of laser drilling, the photoacoustic microscope, laser annealing, fusion phenomena, etc. Several studies [21, 22] based on structures of semiconductors were enacted in the last few decades.

For the first time, Gordon et al. [23] derived the method of photothermal. They introduced the electronic deformations of the photothermal spectroscopy.

The photothermal systems are found to be useful in measuring the electric as well as a temperature effect of semiconductor materials [24–26]. Kreuzer [27] used photoacoustic spectroscopy in the sensitivity analysis. Further, Song et al. [28, 29] presented the generalized thermoelastic vibration of the optically excited semiconducting microcantilevers and the bending of semiconducting cantilevers. Song et al. [30] propounded the reflection of photothermal waves in a semiconducting medium under a generalized theory of thermoelasticity. Lotfy [31] derived the elastic wave motions for a photothermal medium using the dual-phase-lag model in presence of an internal heat source and gravitational field. By adopting the concept of photothermal theory, the two-temperature plane strain problem for a semiconducting medium was analyzed by Abo-Dahab and Lotfy [32]. Moreover, Lotfy and Sarkar [33] applied the definition of memory-dependent derivative for photothermal semiconducting medium in two-temperature generalized thermoelasticity theory. Hobiny and Abbas [34] demonstrated the photothermal waves in an unbounded semiconductor medium with a cylindrical cavity. The photothermal wave in one-dimensional semiconducting material was investigated by [35, 36]. Zenkour [37, 38] discussed a refined multi-phase-lags theory for photothermal waves of a gravitated semiconducting half-space. Recently, Khamis et al. [39] stated a thermal-piezoelectric problem of a semiconductor medium during photo-thermal excitation. Lotfy and Abo-Dahab [40] studied about the two-dimensional problem of two temperature generalized thermoelasticity with normal mode analysis under thermal shock problem. Also the effect of variable thermal conductivity during the photothermal diffusion process of semiconductor medium was shown by Lotfy [41]. Khamiset al. [42] demonstrated the photothermal excitation processes with refined multi dual phase-lags theory for semiconductor elastic medium. Later on, Lotfy et al. [43] published an article about the response of electromagnetic and Thomson effect of semiconductor medium due to laser pulses and thermal memories during photothermal excitation.

Nonlocal continuum theory is attracting the researchers due to its character to investigate the influence of all the points of the material at its single physical point. In the nineteenth-century, Eringen [44–46] proposed the non-local theory to deal with small-scale structure problems. The main idea behind

this theory is that the interacting forces between material points exhibit a far-reaching property. Tzou [11] shows that non-local phenomenon exhibits the same characteristic as the concept of phase lags as phase-lag captures the ultrafast response in femtosecond, non-locality effect reveals the physical mechanism at the nanoscale. Later, Tzou and Guo [47] demonstrated the thermal conduction model which phase-lag and nonlocal responses. Non-local thermoelastic wave propagation in the plates is investigated by Inan and Eringen [48]. Dhaliwal [49] derived the energy equation as well as the work equation in the non-local generalized theory of thermoelasticity. The effect of non-local thermoelasticity on buckling of axially functionally graded nano-beams was introduced by Lei et al. [50]. Lim et al. [51] worked on a higher-order non-local elasticity and strain gradient theory. Tiwari and Kumar [52] investigated the plane wave propagation in non-local thermoelasticity. Othman and Lotfy [53] analysed the effect of rotation on plane waves in generalized thermo-microstretch elastic solid with one relaxation time. Othman and Said [54] investigated 2D problem of magneto-thermoelasticity fiber-reinforced medium under temperature dependent properties with three-phase-lag model. Also, Othman et al. [55] shown the effect of the gravity on the photothermal waves in a semiconducting medium with an internal heat source and one relaxation time. Effect of semiconducting medium with temperature dependent properties under LS and DPL theories was revealed by Othman et al. [56, 57]. Sarkar et al. [58] presented the effect of the laser pulse on transient waves in a non-local thermoelastic medium under Green-Naghdi theory. Propagation of the photothermal waves in a semiconducting medium under L-S theory was given by Othman et al. [59]. Sarkar et al. [60] presented the propagation of photothermal waves using the LS model of thermoelasticity.

Authors' believe that study of photothermal waves in a semiconducting medium in context of dual phase lag thermoelasticity theory with non-local effect has not been performed till now. Therefore, the aim of the present article is to establish a new non-local thermoelastic model in the frame of two relaxation times for the photothermal wave propagation in a semiconducting medium. Analytical results are derived for the field quantities – displacements, stresses, temperature, and carrier density by adopting the method of normal mode

analysis. Computational calculations are rendered for silicon material and graphically presented in the studied physical fields. The results reveal that there are significant effects of the phase lags and non-locality on the thermoelastic interactions inside the semiconductor medium.

2 Formulation of the problem and basic equations

On the basis of theoretical analysis of the heat transport process in a semiconductor, one can retrieve three different types of waves—thermal waves, elastic waves, and coupled plasma waves inside the medium simultaneously. An isotropic homogeneous semiconducting medium has been taken into account (Fig. 1).

Thermal, elastic, and coupled plasma conduction equation for our problem can be written in the following way [25–27, 37]:

$$\mu u_{i,ji} + (\lambda + \mu)u_{i,i} - \gamma T_{,i} - \delta_n N_{,i} = \rho(1 - \xi^2 \nabla^2)u_{,it}, \tag{1}$$

$$K\left(1 + \tau_T \frac{\partial}{\partial t}\right)\nabla^2 T = \left(1 + \tau_q \frac{\partial}{\partial t}\right)(\rho c_v \dot{T} + \gamma T_0 \dot{\epsilon}) - \frac{E_g}{\tau} N, \tag{2}$$

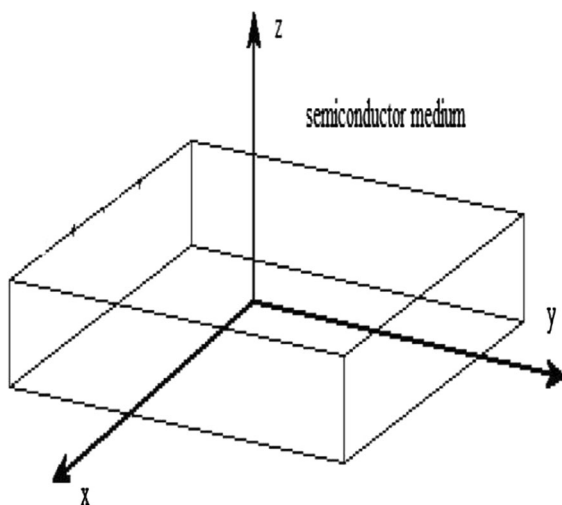


Fig. 1 Schematic representation of semiconducting medium

$$D_E \nabla^2 N - \frac{N}{\tau} + \kappa T = \frac{\partial N}{\partial t}. \tag{3}$$

The constitutive relations are

$$(1 - \xi^2 \nabla^2)\sigma_{ij} = 2\mu e_{ij} + [\lambda e - \gamma T - \delta_n N]\delta_{ij}, \tag{4}$$

$$e_{ij} = \frac{1}{2}(u_{i,j} + u_{j,i}), \quad i, j = 1, 2, 3. \tag{5}$$

$\xi = a_0 e_0$ represents the elastic nonlocal parameter with a dimension of length where a_0, e_0 , denote an internal characteristic length and a material constant, respectively.

Assuming that the direction of the plane strain state is the xy -plane, then the displacement vector u takes the following form

$$u = [u, v, 0](x, y, t) \tag{6}$$

In order to obtain the governing equations into a more convenient form, we introduce the following non-dimensional quantities in the governing equations:

$$\begin{aligned} (x', y', u', v') &= \frac{1}{C_1 \eta}(x, y, u, v), \\ (t', \tau_0') &= \frac{1}{\eta}(t, \tau_0), \quad T' = \frac{\gamma}{(\lambda + 2\mu)}T, \\ N' &= \frac{\delta_n}{(\lambda + 2\mu)}N, \quad \sigma'_{ij} = \frac{1}{\mu}\sigma_{ij}, \\ C_1^2 &= \frac{\lambda + 2\mu}{\rho}, \quad \eta = \frac{K}{\rho c_v C_1^2}. \end{aligned} \tag{7}$$

Displacement components u and v can be written in the terms of displacement potentials $\Phi(x, y, t)$ and $\Psi(x, y, t)$ in the following way

$$u = \Phi_{,x} + \Psi_{,y}, \quad v = \Phi_{,y} + \Psi_{,x} \tag{8}$$

Using Eqs. (6)–(8) in Eqs. (1)–(3), we obtain the following equations in the non-dimensional form (primes are omitted for the sake of simplicity):

$$\left[\left(1 + \xi^2 \frac{\partial^2}{\partial t^2}\right)\nabla^2 - \frac{\partial^2}{\partial t^2}\right]\Phi - T - N = 0, \tag{9}$$

$$\left[\left(1 + \xi^2 \frac{\partial^2}{\partial t^2}\right)\nabla^2 - r_0^2 \frac{\partial^2}{\partial t^2}\right]\Psi = 0, \tag{10}$$

$$\left[\left(1 + \tau_T \frac{\partial}{\partial t} \right) \nabla^2 - \left(\frac{\partial}{\partial t} + \tau_q \frac{\partial^2}{\partial t^2} \right) \right] T - r_1 \left(\frac{\partial}{\partial t} + \tau_q \frac{\partial^2}{\partial t^2} \right) \nabla^2 \Phi + r_2 N = 0, \tag{11}$$

$$\left[\nabla^2 - \frac{K\eta}{\rho c_v \tau D_E} - \frac{K\eta}{\rho c_v D_E} \frac{\partial}{\partial t} \right] N + r_3 T = 0. \tag{12}$$

With the help of Eq. (4), the following expressions of the stress components have been obtained:

$$(1 - \xi^2 \nabla^2) \sigma_{xx} = r_0^2 u_{,x} + (r_0^2 - 2) v_{,y} - r_0^2 T - r_0^2 N, \tag{13}$$

$$(1 - \xi^2 \nabla^2) \sigma_{yy} = (r_0^2 - 2) u_{,x} + r_0^2 v_{,y} - r_0^2 T - r_0^2 N, \tag{14}$$

$$(1 - \xi^2 \nabla^2) \sigma_{xy} = u_{,y} + v_{,x}. \tag{15}$$

Here, $r_0^2 = \frac{\lambda + 2\mu}{\mu}$, $r_1 = \frac{\gamma^2 T_0}{K\eta(\lambda + 2\mu)}$, $r_2 = \frac{\eta E_g \alpha_t}{\rho c_v \tau d_n}$, and $r_3 = \frac{\kappa K \eta d_n}{\rho c_v \alpha_t D_E}$.

3 Solutions of the problem

In order to find the solution of the present problem, we employed normal mode analysis.

Since, harmonic waves are travelling in xy —plane; therefore, all the physical quantities can be decomposed in the following way-

$$f(x, y, t) = f^*(x) e^{\omega t + i b y}. \tag{16}$$

where b is representing the wave number in the y -direction, i reflects the complex quantity, ω is a complex constant and f^* is presenting the amplitude of the field quantity f .

Using transformation (16) in Eqs. (9)–(12), we get

$$\left(\frac{d^2}{dx^2} - p_1 \right) \Phi^* - p_0 T^* - p_0 N^* = 0, \tag{17}$$

$$\left(\frac{d^2}{dx^2} - p_2^2 \right) \Psi^* = 0, \tag{18}$$

$$-p_3 \left(\frac{d^2}{dx^2} - b^2 \right) \Phi^* + \left(\frac{d^2}{dx^2} - p_4 \right) T^* + p_5 N^* = 0, \tag{19}$$

$$r_3 T^* + \left(\frac{d^2}{dx^2} - p_6 \right) N^* = 0. \tag{20}$$

$$p_0 = \frac{1}{1 + \xi^2 \omega^2}, \quad p_1 = b^2 + \frac{\omega^2}{1 + \xi^2 \omega^2}, \quad p_2 = \sqrt{b^2 + \frac{r_0^2 \omega^2}{1 + \xi^2 \omega^2}},$$

$$p_3 = \frac{r_1 \omega (1 + \tau_q \omega)}{(1 + \tau_T \omega)}, \quad p_4 = b^2 + \frac{\omega (1 + \tau_q \omega)}{(1 + \tau_T \omega)}, \quad p_5 = \frac{r_2}{(1 + \tau_T \omega)},$$

$$p_6 = b^2 + \frac{K}{\rho c_v D_E} \left(\omega + \frac{\eta}{\tau} \right).$$

Φ^* , Ψ^* , T^* and N^* represent the amplitudes of Φ , Ψ , T , N , respectively.

For non-trivial solution of Eqs. (17), (19), (20), the determinant of the factor matrix should be equal to zero

$$\begin{vmatrix} \left(\frac{d^2}{dx^2} - p_1 \right) & -p_0 & -p_0 \\ -p_3 \left(\frac{d^2}{dx^2} - b^2 \right) & \left(\frac{d^2}{dx^2} - p_4 \right) & p_5 \\ 0 & r_3 & \left(\frac{d^2}{dx^2} - p_6 \right) \end{vmatrix} = 0. \tag{21}$$

On eliminating $\Phi^*(x)$, $T^*(x)$ and $N^*(x)$ from the Eqs. (17), (19), and (20), we obtain the following decoupled sixth-order ordinary differential equation involving (Φ^*, T^*, N^*) as

$$\left[\frac{d^6}{dx^6} - A \frac{d^4}{dx^4} + B \frac{d^2}{dx^2} - C \right] \{ \Phi^*(x), T^*(x), N^*(x) \} = 0, \tag{22}$$

where $A = p_1 + p_0 p_3 + p_4 + p_6$, $B = p_1 (p_4 + p_6) + p_0 p_3 (b^2 + p_6 + r_3) + p_4 p_6 - r_3 p_5$, $C = p_1 (p_4 p_6 - r_3 p_5) + p_0 p_3 b^2 (p_6 + r_3)$.

After factorizing, Eq. (22) can be expressed as

$$\left(\frac{d^2}{dx^2} - \beta_1^2 \right) \left(\frac{d^2}{dx^2} - \beta_2^2 \right) \left(\frac{d^2}{dx^2} - \beta_3^2 \right) \{ \Phi^*(x), T^*(x), N^*(x) \} = 0, \tag{23}$$

where β_i^2 ($i = 1, 2, 3$) denote the roots of the following characteristic equation

$$\beta^6 - A\beta^4 + B\beta^2 - C = 0. \tag{24}$$

The solution of Eq. (23) which is bounded for $x \rightarrow \infty$, is obtained as

$$\Phi^*(x) = \sum_{n=1}^3 M_n e^{-\beta_n x}, \tag{25}$$

$$T^*(x) = \sum_{n=1}^3 H_{1n} M_n e^{-\beta_n x}, \tag{26}$$

$$N^*(x) = \sum_{n=1}^3 H_{2n} M_n e^{-\beta_n x}. \tag{27}$$

The solution of Eq. (18) can be written as

$$\Psi^*(x) = M_4 e^{-p_2 x}. \tag{28}$$

Here, M_n ($n = 1, 2, 3, 4$) are representing the coefficients and $H_{1n} = \frac{(\beta_n^2 - p_1)(\beta_n^2 - p_6)}{p_0(\beta_n^2 - p_6) - r_3}$, $H_{2n} = \frac{r_3 H_{1n}}{p_6 - \beta_n^2}$.

Using Eqs. (8), (16), (25), and (28), we obtain the following analytical expressions of the components of the displacement

$$u^* = \sum_{n=1}^3 M_n e^{-\beta_n x} + i b M_4 e^{-p_2 x}, \tag{29}$$

$$v^* = \sum_{n=1}^3 i b M_n e^{-\beta_n x} + p_2 M_4 e^{-p_2 x}. \tag{30}$$

Using Eqns. (13)–(16) and (25)–(30), exact analytical expressions of the components of the stress can be expressed as

$$\sigma_{xx}^* = \sum_{n=1}^3 H_{3n} M_n e^{-\beta_n x} - H_{34} M_4 e^{-p_2 x}, \tag{31}$$

$$\sigma_{yy}^* = \sum_{n=1}^3 H_{4n} M_n e^{-\beta_n x} + H_{34} M_4 e^{-p_2 x}, \tag{32}$$

$$\sigma_{xy}^* = - \sum_{n=1}^3 H_{6n} M_n e^{-\beta_n x} - H_{64} M_4 e^{-p_2 x}. \tag{33}$$

where

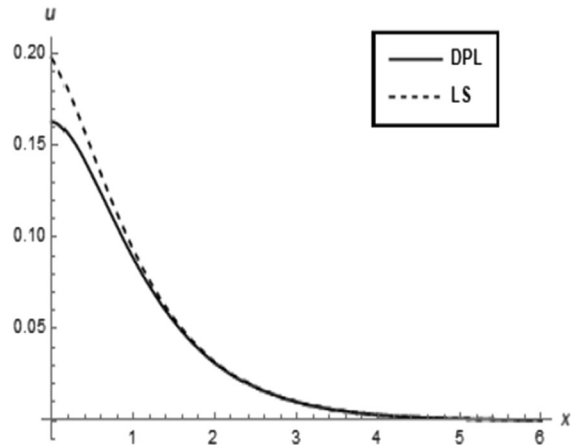


Fig. 2 Distribution of horizontal displacement u with distance x

$$\begin{pmatrix} M_1 \\ M_2 \\ M_3 \\ M_4 \end{pmatrix} = \begin{pmatrix} H_{31} & H_{32} & H_{33} & -H_{34} \\ H_{61} & H_{62} & H_{63} & H_{64} \\ \beta_1 H_{11} & \beta_2 H_{12} & \beta_3 H_{13} & 0 \\ (\beta_1 + s_1) H_{21} & (\beta_2 + s_1) H_{22} & (\beta_3 + s_1) H_{23} & 0 \end{pmatrix}^{-1} \begin{pmatrix} -m_1^* \\ 0 \\ 0 \\ 0 \end{pmatrix} \tag{34}$$

$$s_1 = \frac{s}{D_E}$$

4 Boundary conditions

We have to choose the values of the coefficients M_n ($n = 1, 2, 3, 4$) in such a way so that the boundary conditions on the surface $x = 0$ take the form

$$\sigma_{xx} = -m_1 = -m_1^* e^{i\omega t + i b y}, \quad \sigma_{xy} = 0, \tag{35}$$

$$\frac{\partial T}{\partial x} = 0 \quad D_E \frac{dN}{dx} = sN.$$

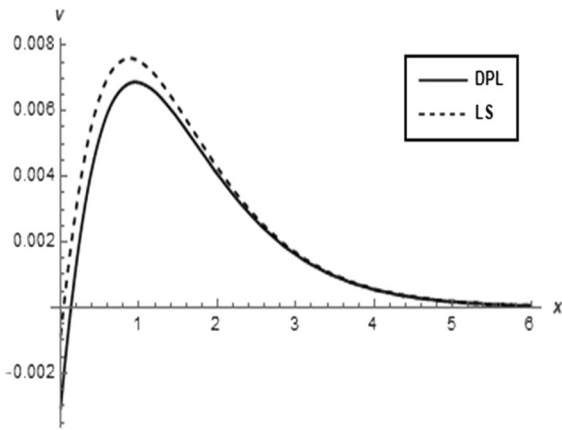


Fig. 3 Distribution of vertical displacement v with distance x

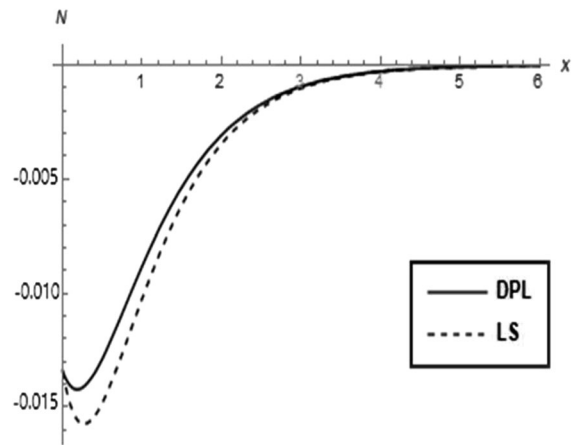


Fig. 5 Distribution of carrier density N with distance x

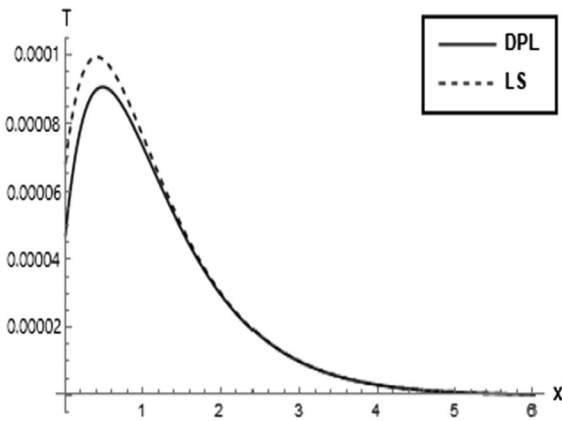


Fig. 4 Distribution of temperature T with distance x

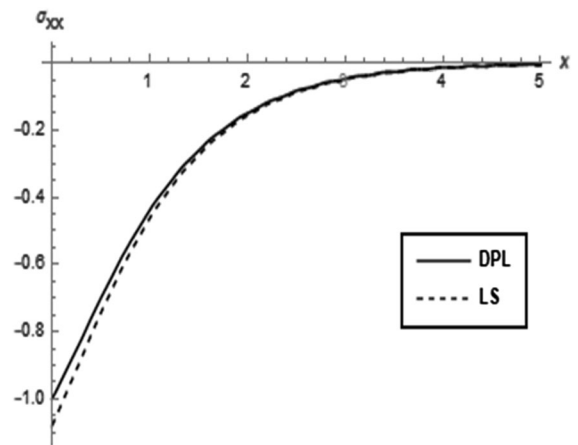


Fig. 6 Distribution of stress component σ_{xx} with distance x

m_1^* and s are constants.

Applying the boundary conditions (35) at the surface $x = 0$, we obtain a system of four equations and we find the values of the coefficients M_n ($n = 1, 2, 3, 4$) by adopting the inversion of the matrix of order four in the following way

$$\begin{pmatrix} M_1 \\ M_2 \\ M_3 \\ M_4 \end{pmatrix} = \begin{pmatrix} H_{31} & H_{32} & H_{33} & -H_{34} \\ H_{61} & H_{62} & H_{63} & H_{64} \\ \beta_1 H_{11} & \beta_2 H_{12} & \beta_3 H_{13} & 0 \\ (\beta_1 + s_1)H_{21} & (\beta_2 + s_1)H_{22} & (\beta_3 + s_1)H_{23} & 0 \end{pmatrix}^{-1} \begin{pmatrix} -m_1^* \\ 0 \\ 0 \\ 0 \end{pmatrix} \tag{36}$$

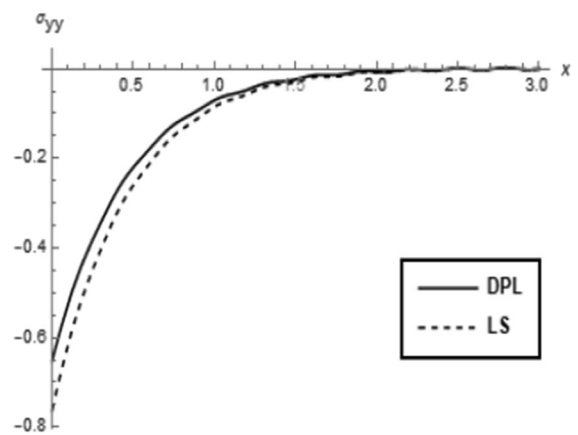


Fig. 7 Distribution of stress component σ_{yy} with distance x

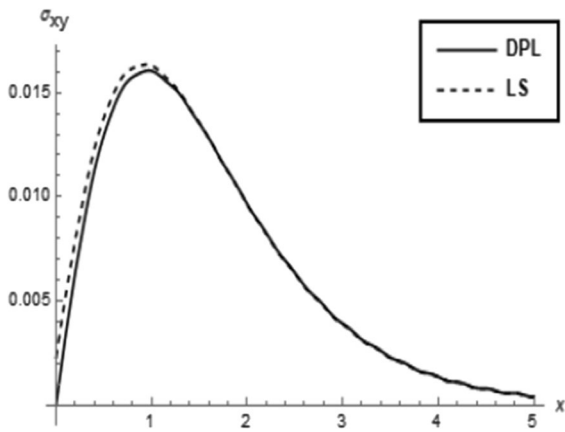


Fig. 8 Distribution of stress component σ_{xy} with distance x

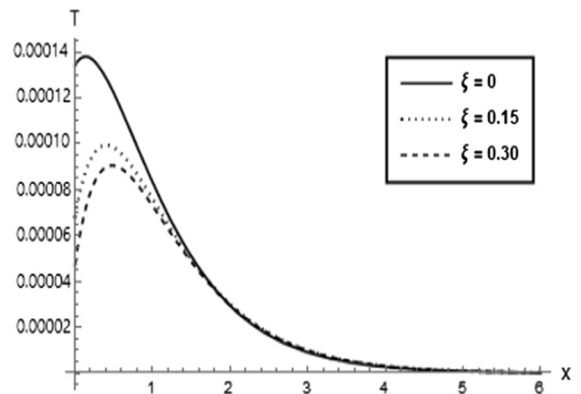


Fig. 11 Distribution of temperature T with distance x

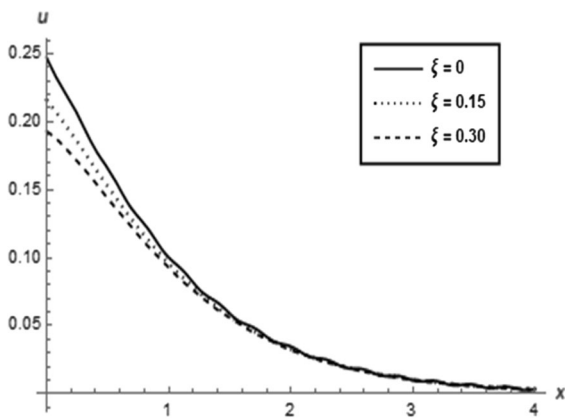


Fig. 9 Distribution of horizontal displacement u with distance x

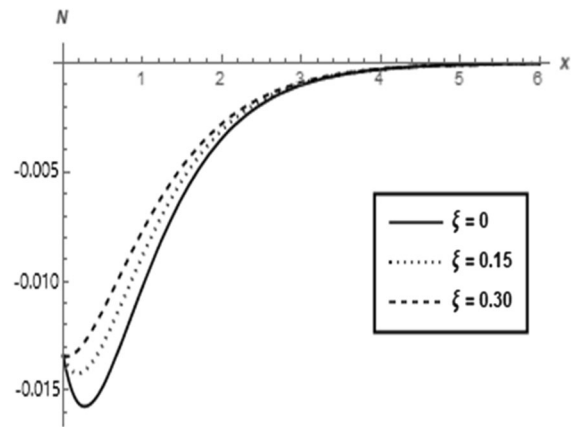


Fig. 12 Distribution of carrier density N with distance x

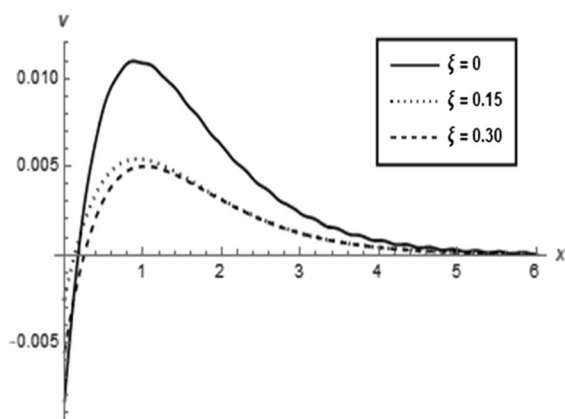


Fig. 10 Distribution of vertical displacement v with distance x

$$s_1 = \frac{s}{D_E}$$

5 Numerical results

The previous section exhibits the analytical solutions of the field quantities – displacement components, temperature, stress components, and carrier density. In order to predict the clear picture of these field quantities, present section aims to determine the numerical results of the field quantities for the non-dimensional time $t = 0.05$.

The graphical results have been examined in two separate groups. The first group reveals the difference between two the theories of heat conduction—single

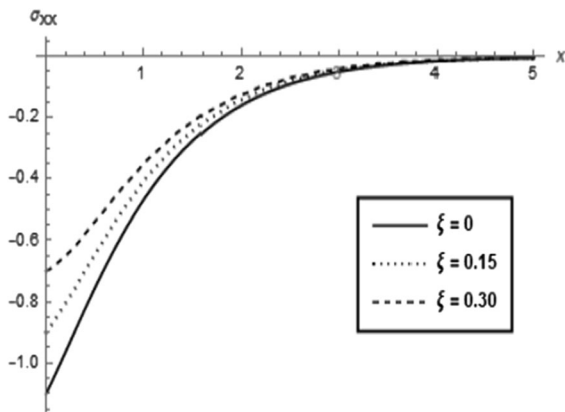


Fig. 13 Distribution of stress component σ_{xx} with distance x

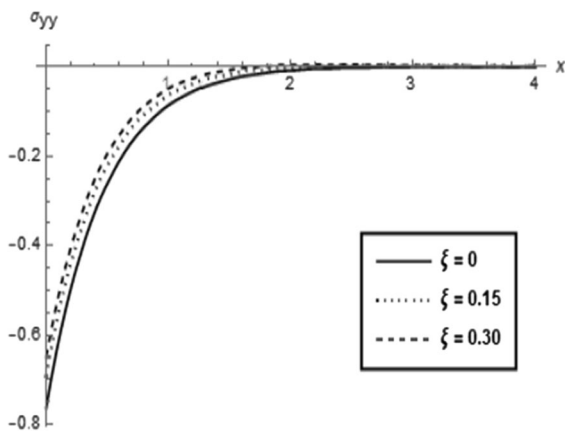


Fig. 14 Distribution of stress component σ_{yy} with distance x

phase lag theory (LS model) and dual phase lag theory (DPL model) so that the effect of the phase lags on the behavior of different field quantities has been characterized (Figs. 1, 2, 3, 4, 5, 6, 7). The second group describes the influence of the non-local elastic parameter ξ on the behavior of different physical fields (Figs. 8, 9, 10, 11, 12, 13, 14).

For numerical simulation, Silicon material has been selected. The physical parameters for Silicon are assumed as [25, 46, 47]:

$$\lambda = 3.64 \times 10^{10} Nm^{-2}, \quad \mu = 5.46 \times 10^{10} kgm^{-1}s^{-2},$$

$$\alpha_t = 3 \times 10^{-6} k^{-1}, \quad K = 150 wm^{-1}k^{-1}, \quad s = 2ms^{-1}, \quad \rho = 2.33 \times 10^3 kgm^{-3},$$

$$c_v = 695 Jkg^{-1}k^{-1}, \quad b = 1.2, \quad T_0 = 300 K, \quad m_1^* = 1, \quad \tau = 5 \times 10^{-5},$$

$$\omega = \omega_0 + i\xi, \quad \omega_0 = 1, \quad \xi = 0.03, \quad r_3 = -450,$$

$$D_E = 2.5 \times 10^{-3} m^2s^{-1}, \quad d_n = -9 \times 10^{-31} m^3, \quad E_g = 1.12 eV,$$

$$\tau_T = 0.03, \quad \tau_q = 0.04, \quad y = 0.05.$$

The physical data outlined above has been used to calculate the distributions of the real part of the horizontal displacement component u , vertical displacement component v , the temperature T , the carrier density N , and the stress components σ_{xx} , σ_{yy} , and σ_{xy} . All the physical variables are considered in non-dimensional form.

5.1 Effect of phase lags

Figure 2 demonstrates the behaviour of the horizontal component u of the displacement against the distance x for the non-dimensional time $t = 0.05$. It can be observed from Fig. 2 that the displacement curves for dual-phase-lag (DPL) and single-phase-lag (LS) models start from the surface of the semiconducting medium with the positive values and gradually decreases in the direction of the increasing distance and vanish around the range $4 \leq x \leq 5$. But we observe that the curve representing single phase lag model i.e. LS model differs in the highest manner at the beginning from the curve representing dual phase lag model i.e. DPL model and this difference decreases as the values of the distance increases and the difference becomes negligible for the value of the distance greater than 2. It may be noticed from the above figure, dual phase lag model of heat conduction suppresses the values of the component of displacement which implies the less dissipation of energy and consequently provides the waves of less attenuation compared to the LS model of heat conduction with single phase lag. This nature of the horizontal component u of the displacement shows that the insertion of phase lag in the heat conduction equation has a very prominent influence on the horizontal component of the displacement field.

Figure 3 characterizes the variations of the vertical component v of the displacement versus the distance x . In contrast with the horizontal component u , vertical component v begins from the negative value at the boundary of the semiconducting medium and moves towards the positive direction as the distance increases for $(0 \leq x \leq 1.5)$. After reaching a peak value in the positive direction, the curves start to decrease as the distance increases for $(1.5 < x \leq 6)$ and fade away after passing the distance nearer to 6. Impact of the phase lags is noticed to be more prominent on the vertical component of the displacement field and we observe that the addition of the relaxation times in the heat conduction equation decreases

the values of the vertical component and this effect is observed to be most significant at the peak value.

One remarkable point is noticed that horizontal and vertical both components of the displacement field vanish at the bounded region which shows the finite speed of thermoelastic waves.

Figure 4 describes the variations of the temperature profiles against the distance for DPL and LS models. The trend of the variation of the temperature profile begins from a constant value on the boundary of the semiconducting medium but it increases for small values of the distance nearer to 1 and starts decreasing after crossing the distance equal to 1 and reaches to zero at the distance nearer to 5. Constant nature of temperature field at the boundary of the semiconducting medium satisfies the boundary condition. Similar to the displacement profiles, the values of the temperature are found to be higher for the Lord-Shulman (LS) model compared to the corresponding profile of dual phase lag model. The influence of phase lags is most prominent at the maximum value of the temperature. Attractiveness of dual phase lag model can be understood in such a way that high values of temperature increases thermal stress inside the medium which may reduce the structural ability of the material.

Figure 5 states the nature of the carrier density with respect to the distance for DPL and LS models. The profiles of the carrier density start from the negative value on the boundary of the medium and goes towards the positive direction exponentially and ultimately reaches zero. This distributions of carrier density is observed to be continuous, smooth and exponential function satisfying the boundary condition. This kind of propagation mode satisfies the elastic properties of semiconducting materials. It is noticed from the figure that the curve representing the LS model differs in the beginning from the curve of the dual-phase-lag model, but after passing some distance nearer to 4 and inside the semiconducting medium, the curves converge until they all fade. An important observation that can be observed from the figure is that the profile of the carrier density in the case of the Lord-Shulman (LS) model is spread and faded faster than in the case of the dual-phase-lag (DPL) model. This figure also shows that the presence of the phase lags is influential in the propagation of the waves.

Figure 6 presents the variations of the stress component σ_{xx} distributions with respect to the distance for LS and DPL models. Starting from a negative value on the boundary of the semiconducting medium, the stress profile moves towards the positive direction and finally reaches to zero. The effect of phase lags is clearly visible in the profiles of the stress distribution. This effect is significant at the beginning and as the distance passes, both curves converge and vanish nearer the distance $x = 3$.

Further, an important point comes from the figure that the stress profile under dual phase lag (DPL) model shows lower stress compared to the stress profile for the Lord-Shulman model (LS model). Hence, we can conclude that the waves in context of dual phase lag model are less attenuated as they dissipate less amount of energy due to low values of thermal stress compared to the LS model of heat conduction. In this way, dual phase lag model proves itself a better model for the physical system.

Figure 7 depicts the variations of the stress component σ_{yy} with respect to the distance for LS and DPL models. Similar to Fig. 6, the curves representing the stress component σ_{yy} start from a negative value on the boundary of the medium and then move towards the positive direction and after passing some distance, the profiles disappear. It is noticed that the domain of influence is greater for Lord and Shulman model compared to the corresponding profile of dual phase lag model and therefore it can be concluded that the dual phase lag model is found to be more efficient compared to the Lord-Shulman model.

Figure 8 indicates the nature of the stress component σ_{xy} versus the distance for Lord Shulman and the dual phase lag models. Unlike the Figs. 6, 7, 8 shows that the values of the stress profile are always positive. The trend of variation of the profile is such that it starts from a very small value close to zero but it increases as the distance increases and after providing a peak value, it starts decreasing and ultimately vanishes for the higher values of the distance. Here, the Lord-Shulman model predicts higher values of stress compared to the stress profile for dual phase lag model. Thus, it can be concluded again that the role of phase lag is strongly visible on the variations of each field quantity.

5.2 Effect of elastic non-local parameter

The variations of the distribution of displacement component u versus the distance x are presented in Fig. 9, which provides the values of the displacement component for the non-local and local dual phase lag (DPL) models. The figure shows the effect of the elastic non-local parameter ξ on the displacement behavior. The case $\xi=0$ represents the case of the local DPL model and non-zero values of ξ exhibit the non-local DPL model. Starting from a constant value at the boundary of the semiconducting medium, displacement profiles begin to decrease as the distance increases. It is observed from the figure that the displacement component has the maximum value on the boundary of the semiconducting medium. Further, we observe that the profile representing the local theory differs at the beginning from the profiles of the non-local theory, but after passing the distance and inside the material the curves converge until they all vanish. An important observation that can be obtained from the figure is that the wave propagation in the case of the non-local theory fades faster compared to the local one. Moreover, we find a piece of important information from the figure that for a higher value of the elastic non-local parameter exhibits low values of the displacement compared to the profiles having a low value of an elastic non-local parameter. This result shows the adorableness of the insertion of non-local parameter on the governing equations.

Figure 10 displays the variation of the distribution of displacement component v versus the distance x which gives the values of the displacement component for the non-local and local dual phase lag (DPL) models. The figure shows the effect of the elastic non-local parameter ξ on the behaviour of the displacement component v . Here, the trend of variation of the vertical component of displacement profile is found to be different compared to the profile of the horizontal component of the displacement profile. Starting from a negative value, the profile of the vertical component of the displacement moves towards the positive values and after reaching a maximum value it goes down as the distance achieves a higher value. It is visible that the influence of elastic non-local parameters are much prominent on the profiles of the vertical displacement. This influence is found to be highest at the maximum value. Further, we observe that the profile representing the local theory has the greatest domain

of influence and the domain of influence of the profile decreases when an elastic non-local parameter has a non-zero value. Similar to the profiles of horizontal displacement, vertical displacement in the case of the non-local theory fades faster compared to the local one. Moreover, we find important information from the figure that the higher value of the elastic non-local parameter predicts low values of the displacement. Here, the values of the displacement component differ in the significant way when non-local parameter is found to be absent and in this way absence of non-local parameter become a big cause of high energy loss.

Figure 11 displays the characteristics of the temperature with respect to the distance for the local and non-local dual phase lag model. The influence of the elastic non-local parameter ξ on the temperature distribution has been analyzed by assuming different values which are 0, 0.15, and 0.30. The case of $\xi = 0$, corresponds to the case of the local dual phase lag model. Non-zero values of elastic non-local parameter ξ , represent the non-local dual phase lag model.

It is noticed from Fig. 11 that the temperature profiles begin at the surface of the semiconducting medium with very small values 1 and then they increase until they reach their maximum value and then steadily decrease in the direction of increasing the distance until it approaches zero. The temperature values for the non-local dual phase lag model ($\xi > 0$) are smaller than those for the local dual phase lag model ($\xi = 0$). This result implies that the effects of non-locality reduce the values of the temperature and when the value of the non-local elastic parameter increases, the values of the temperature decrease, and therefore the domain of influence of the temperature profile decreases for the higher value of the elastic non-local parameter. Moreover, the differences between local and non-local are found to be more significant initially (for small values of the distance).

Figure 12 refers to the behaviour of the carrier density versus the distance for the local and non-local dual phase lag model. From Fig. 12, it is observed that the profiles start from a negative value, move towards the positive direction, and ultimately disappear. The maximum rate of decay is found in the range $0.4 \leq x \leq 4$. An important fact comes from the figure that the profiles of the non-local model fade earlier compared to the local one. Further, the profile under the local dual phase lag model provides

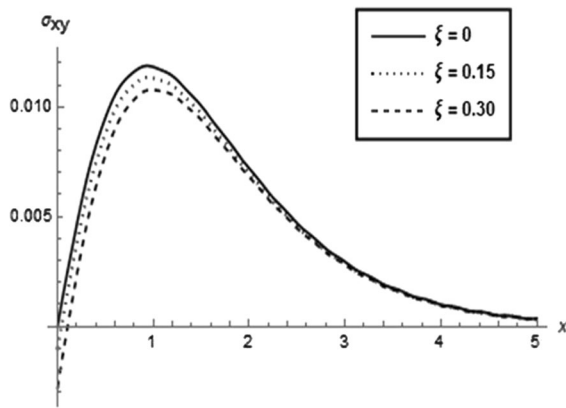


Fig. 15 Distribution of stress component σ_{xy} with distance x

minima. Similar to the previous figures, the effect of non-locality decreases the values of the profiles of carrier density also.

Figure 13 clarifies the variations of the stress component σ_{xx} with respect to the distance for the non-local and local dual-phase-lag models. Profiles of stress start from a negative value on the boundary of the semiconducting medium then move towards the positive direction and finally reaches to zero. Non-local effect is found to be similar to previous figures and the difference between non-local and local is found to be prominent in the initial stage, later, the profiles of stress converge and vanish for the distance nearer to 4. This Figure supports the efficiency of the non-local model compared to the local one as stress is found to be very less under the non-locality effect compared to the local model.

Figure 14 states the variations of the stress component σ_{yy} against the distance for non-local and local dual phase lag model. The trend of variations of σ_{yy} resembles with the σ_{xx} . However, the values of the stress component σ_{yy} are higher compared to the corresponding values of the stress component σ_{xx} . The effect of non-locality is similar to Fig. 13 but this effect is less compared to the previous figure (Fig. 13). But, this figure also clarifies that the non-local model is more effective and capable to predict better results compared to the local model.

Figure 15 visualizes the variations of the stress component σ_{xy} against the distance for non-local and local dual phase lag model. In this case, the values of the stress are found to be positive. The influence of

the non-locality effect reduces the values of the stress and proves itself better compared to the local model.

6 Conclusions

The motive of the present work is to develop a new non-local thermoelastic model in the frame of two phase lags for photothermal wave propagation. A semiconducting medium has been assumed to study photothermal waves. The analytical solutions have been obtained by adopting the method of normal mode analysis which covers a wide range of problems in thermoelasticity. This method is capable to provide exact solutions without any assumed restrictions on the actual physical quantities that appear in the governing equations of the physical problem considered. The effect of significantly different parameters, such as non-local elastic parameters and the presence of phase lags on different distributions, has been analyzed. Thorough discussion and study, the following conclusions are revealed-

1. Distributions of all physical quantities such as horizontal and vertical components of the displacement, temperature, carrier density, and thermal stress appear clearly in a limited region near the surface of the semiconducting medium and these effects gradually disappear outside this region after a certain period of time. This physical phenomenon demonstrates the fact that photothermal waves propagate at a finite speed inside the medium contrary to the traditional theories which predict the infinite speed of the thermal wave.
2. The profiles representing the distributions of field quantities- temperature, components of the displacement, carrier density, and components of the stress temperature vanish earlier for higher values of the non-local elastic parameter. However when the non-local elastic parameter is consider to be zero i.e. all the field quantities obtain higher values which become an important reason of high dissipation of energy. High values of temperature generate high values of thermal stress which may reduce the structural ability of the material. This result concludes that the non-local dual-phase-lag

model proves itself a more efficient model compared to the case of without non-local effect.

3. When the results are compared to the corresponding results predicted by the Lord-Shulman model, we observe that the results under the purview of dual-phase-lag model attain lower values as compared to the results predicted by the Lord-Shulman model. This result implies that the role of phase lags in the heat conduction equation is found to be very significant. Insertion of phase lags reduces the values of the field quantities and proves itself a better and more accurate model.
4. All the field quantities are found to be continuous and smooth in nature.
5. It can further be concluded that the non-local parameter exhibits important effects that prove the non-local thermoelasticity model different and more realistic than other previous models. Moreover, the insertion of phase lags makes the heat conduction model more accurate and realistic.
6. We believe that the present investigation will provide important pieces of information for the development of more accurate and realistic non-local thermoelastic mathematical models in modern technology.

For industrial purpose especially in microelectronic devices, excitation of thermal waves in semiconductor materials exhibit prominent role. This type of study can be beneficial for the design and analysis of the thermal, plasma and a pulsed laser coated materials, and several various engineering practices related to interface analysis and design.

There are many applications of photo-thermal excitation in a semiconducting medium. Present investigation can be incorporated in the designs of actuators, transducers, resonators, filters, sensors and electric circuits

Declarations

Conflict of interest Author(s) have no any potential conflict of interest.

References

1. Biot MA (1956) Thermoelasticity and irreversible thermodynamics. *J Appl Phys* 27:240. <https://doi.org/10.1063/1.1722351>
2. Lord HW, Shulman Y (1967) A generalized dynamical theory of thermoelasticity. *J Mech Phys Solids* 15:299–309. [https://doi.org/10.1016/0022-5096\(67\)90024-5](https://doi.org/10.1016/0022-5096(67)90024-5)
3. Green AE, Lindsay KA (1972) Thermoelasticity. *J Elast* 2:1–7
4. Dhaliwal RS, Sherief HH (1980) Generalized thermoelasticity for anisotropic media. *Q Appl Math*. <https://doi.org/10.1090/qam/575828>
5. Green AE, Naghdi PM (1991) A re-examination of the basic postulates of thermomechanics. *Proc R Soc A Math Phys Eng Sci* 432:171–194. <https://doi.org/10.1098/rspa.1991.0012>
6. Green AE, Naghdi PM (1992) On undamped heat waves in an elastic solid. *J Therm Stress* 15:253–264
7. Green AE, Naghdi PM (1993) Thermoelasticity without energy dissipation. *J Elast* 31:189–208. <https://doi.org/10.1007/BF00044969>
8. Tiwari R, Mukhopadhyay S (2017) On electromagneto-thermoelastic plane waves under Green-Naghdi theory of thermoelasticity-II. *J Therm Stress* 40:1040–1062. <https://doi.org/10.1080/01495739.2017.1307094>
9. Kumar R, Kumar R (2019) A study of thermoelastic damping in micromechanical resonators under unified generalized thermoelasticity formulation. *Noise Vib Worldw* 50:169–175. <https://doi.org/10.1177/0957456519853814>
10. Tzou DY (1995) A unified field approach for heat conduction from macro- to micro-scales. *J Heat Transf* 117:8–16. <https://doi.org/10.1115/1.2822329>
11. Tzou DY (2014) Macro- to microscale heat transfer: the lagging behavior (2014)
12. Chandrasekharalah DS (1986) Thermoelasticity with second sound: a review. *Appl Mech Rev* 39:355–376. <https://doi.org/10.1115/1.3143705>
13. Chandrasekharalah DS (1998) Hyperbolic thermoelasticity: a review of recent literature. *Appl Mech Rev* 51:705–729. <https://doi.org/10.1115/1.3098984>
14. Kumar R, Kumar R, Kumar H (2018) Effects of phase-lag on thermoelastic damping in micromechanical resonators. *J Therm Stress*. <https://doi.org/10.1080/01495739.2018.1469061>
15. Kumar R (2020) Effect of phase-lag on thermoelastic vibration of Timoshenko beam. *J Therm Stress* 43:1337–1354. <https://doi.org/10.1080/01495739.2020.1783412>
16. Tiwari R, Misra JC (2020) Magneto-thermoelastic excitation induced by a thermal shock: a study under the purview of three phase lag theory. *Waves Random Complex Media*. <https://doi.org/10.1080/17455030.2020.1800861>
17. Kumar R, Tiwari R, Kumar R (2020) Significance of memory-dependent derivative approach for the analysis of thermoelastic damping in micromechanical resonators. *Mech Time-Depend Mater*. <https://doi.org/10.1007/s11043-020-09477-7>

18. El-Karamany AS, Ezzat MA (2014) On the dual-phase-lag thermoelasticity theory. *Meccanica* 49:79–89. <https://doi.org/10.1007/s11012-013-9774-z>
19. Magaña A, Quintanilla R (2018) On the existence and uniqueness in phase-lag thermoelasticity. *Meccanica* 53:125–134. <https://doi.org/10.1007/s11012-017-0727-9>
20. Rezazadeh G, Sheikhlou M, Shabani R (2015) Analysis of bias DC voltage effect on thermoelastic damping ratio in short nano-beam resonators based on nonlocal elasticity theory and dual-phase-lagging heat conduction model. *Meccanica* 50:2963–2976. <https://doi.org/10.1007/s11012-015-0171-7>
21. Alzahrani FS, Abbas IA (2018) Photo-thermoelastic interactions in a 2D semiconducting medium. *Eur Phys J Plus* 133:1–17. <https://doi.org/10.1140/epjp/i2018-12285-5>
22. Hobiny A, Abbas I (2020) Fractional order GN model on photo-thermal interaction in a semiconductor plane. *Silicon*, 1–8. doi:<https://doi.org/10.1007/s12633-019-00292-5>
23. Gordon JP, Leite RCC, Moore RS, Porto SPS, Whinnery JR (1965) Long-transient effects in lasers with inserted liquid samples. *J Appl Phys* 36:3–8. <https://doi.org/10.1063/1.1713919>
24. Kliger DS (1985) Ultrasensitive laser spectroscopy. *Phys Teach*. <https://doi.org/10.1119/1.2341726>
25. Tam AC (1986) Applications of photoacoustic sensing techniques. *Rev Mod Phys* 58:381. <https://doi.org/10.1103/RevModPhys.58.381>
26. Tam AC (1989) Photothermal investigations of solids and fluids
27. Kreuzer LB (1971) Ultralow gas concentration infrared absorption spectroscopy. *J Appl Phys* 42:2934–2943. <https://doi.org/10.1063/1.1660651>
28. Song Y, Todorovic DM, Cretin B, Vairac P (2010) Study on the generalized thermoelastic vibration of the optically excited semiconducting microcantilevers. *Int J Solids Struct* 47:1871–1875. <https://doi.org/10.1016/j.ijsolstr.2010.03.020>
29. Song Y, Todorovic DM, Cretin B, Vairac P, Xu J, Bai J (2014) Bending of semiconducting cantilevers under photothermal excitation. *Int J Thermophys* 35:305–319. <https://doi.org/10.1007/s10765-014-1572-x>
30. Song YQ, Bai JT, Ren ZY (2012) Study on the reflection of photothermal waves in a semiconducting medium under generalized thermoelastic theory. *Acta Mech* 223:1545–1557. <https://doi.org/10.1007/s00707-012-0677-1>
31. Lotfy K (2016) The elastic wave motions for a photothermal medium of a dual-phase-lag model with an internal heat source and gravitational field. *Can J Phys* 94:400–409. <https://doi.org/10.1139/cjp-2015-0782>
32. Abo-Dahab SM, Lotfy K (2017) Two-temperature plane strain problem in a semiconducting medium under photothermal theory. *Waves Random Complex Media* 27:67–91. <https://doi.org/10.1080/17455030.2016.1203080>
33. Lotfy K, Sarkar N (2017) Memory-dependent derivatives for photothermal semiconducting medium in generalized thermoelasticity with two-temperature. *Mech Time-Depend Mater* 21:519–534. <https://doi.org/10.1007/s11043-017-9340-5>
34. Hobiny AD, Abbas IA (2017) A study on photothermal waves in an unbounded semiconductor medium with cylindrical cavity. *Mech Time-Depend Mater* 21:61–72. <https://doi.org/10.1007/s11043-016-9318-8>
35. Abbas IA, Aly KA, Alzahrani FS (2017) A two-temperature photothermal interaction in a semiconducting material. *J Adv Phys* 6:402–407. <https://doi.org/10.1166/jap.2017.1350>
36. Abbas IA, Aly KA (2017) A generalized model on plasma, thermal and elastic waves in a semiconductor medium. *J Adv Phys* 6:317–325. <https://doi.org/10.1166/jap.2017.1349>
37. Zenkour AM (2019) Refined multi-phase-lags theory for photothermal waves of a gravitated semiconducting half-space. *Compos Struct* 212:346–364. <https://doi.org/10.1016/j.compstruct.2019.01.015>
38. Zenkour AM (2019) Effect of thermal activation and diffusion on a photothermal semiconducting half-space. *J Phys Chem Solids* 132:56–67. <https://doi.org/10.1016/j.jpcs.2019.04.011>
39. Khamis AK, Lotfy K, El-Bary AA, Mahdy AMS, Ahmed MH (2020) Thermal-piezoelectric problem of a semiconductor medium during photo-thermal excitation. *Waves Random Complex Media*. <https://doi.org/10.1080/17455030.2020.1757784>
40. Lotfy K, Abo-Dahab SM (2015) Two-dimensional problem of two temperature generalized thermoelasticity with normal mode analysis under thermal shock problem. *J Comp Theor Nanosci* 12(8):1709–1719
41. Lotfy K (2019) Effect of variable thermal conductivity during the photothermal diffusion process of semiconductor medium. *SILICON* 11(4):1863–1873
42. Khamis AK, El-Bary AA, Lotfy K, Bakali A (2020) Photothermal excitation processes with refined multi dual phase-lags theory for semiconductor elastic medium. *Alex Eng J* 59(1):1–9
43. Lotfy K, Hassan W, El-Bary AA, Kadry MA (2020) Response of electromagnetic and Thomson effect of semiconductor medium due to laser pulses and thermal memories during photothermal excitation. *Results Phys* 16:102877
44. Eringen AC (1972) Nonlocal polar elastic continua. *Int J Eng Sci* 10:1–16. [https://doi.org/10.1016/0020-7225\(72\)90070-5](https://doi.org/10.1016/0020-7225(72)90070-5)
45. Eringen AC (1974) Theory of nonlocal thermoelasticity. *Int J Eng Sci* 12:1063–1077. [https://doi.org/10.1016/0020-7225\(74\)90033-0](https://doi.org/10.1016/0020-7225(74)90033-0)
46. Eringen AC (2002) *Nonlocal continuum field theories* (Springer New York, New York, NY, 2002) doi:<https://doi.org/10.1007/b97697>
47. Tzou DY, Guo ZY (2010) Nonlocal behavior in thermal lagging. *Int J Therm Sci* 49:1133–1137. <https://doi.org/10.1016/j.ijthermalsci.2010.01.022>

48. Inan E, Eringen AC (1991) Nonlocal theory of wave propagation in thermoelastic plates. *Int J Eng Sci* 29:831–843. [https://doi.org/10.1016/0020-7225\(91\)90005-N](https://doi.org/10.1016/0020-7225(91)90005-N)
49. Dhaliwal J (1993) Uniqueness in generalized nonlocal thermoelasticity. *J Therm Stress* 16:71–77. <https://doi.org/10.1080/01495739308946217>
50. Lei J, He Y, Li Z, Guo S, Liu D (2019) Effect of nonlocal thermoelasticity on buckling of axially functionally graded nanobeams. *J Therm Stress* 42:526–539. <https://doi.org/10.1080/01495739.2018.1536866>
51. Lim CW, Zhang G, Reddy JN (2015) A higher-order nonlocal elasticity and strain gradient theory and its applications in wave propagation. *J Mech Phys Solids* 78:298–313. <https://doi.org/10.1016/j.jmps.2015.02.001>
52. Tiwari R, Kumar R (2021) Analysis of plane wave propagation under the purview of three phase lag theory of thermoelasticity with non-local effect. *Eur J Mech/A Solids* 88:104235. <https://doi.org/10.1016/j.euromechsol.2021.104235>
53. Othman MIA, Lotfy K (2011) Effect of rotation on plane waves in generalized thermo-microstretch elastic solid with one relaxation time. *Multidiscipline Modeling in Materials and Structures*
54. Othman MIA, Said SM (2014) 2D problem of magneto-thermoelasticity fiber-reinforced medium under temperature dependent properties with three-phase-lag model. *Meccanica* 49(5):1225–1241
55. Othman MIA, Tantawi RS, Eraki EE (2017) Effect of the gravity on the photothermal waves in a semiconducting medium with an internal heat source and one relaxation time. *Waves Random Complex Media* 27(4):711–731
56. Othman MIA, Tantawi RS, Eraki EE (2017) Effect of rotation on a semiconducting medium with two-temperatures under LS theory. *Arch Thermodyn* 38(2)
57. Othman MIA, Tantawi RS, Eraki EE (2017) Effect of initial stress on a semiconductor material with temperature dependent properties under DPL model. *Microsyst Technol* 23(12):5587–5598
58. Sarkar N, Mondal S, Othman MIA (2020) Effect of the laser pulse on transient waves in a non-local thermoelastic medium under Green-Naghdi theory. *Struct Eng Mech* 74(4):471–479
59. Othman MIA, Tantawi RS, Eraki EEM (2016) Propagation of the photothermal waves in a semiconducting medium under L-S theory. *J Therm Stress* 39:1419–1427. <https://doi.org/10.1080/01495739.2016.1216063>
60. Sarkar N, Mondal S, Othman MIA (2020) L-S theory for the propagation of the photo-thermal waves in a semiconducting nonlocal elastic medium. *Waves Random Complex Media*. <https://doi.org/10.1080/17455030.2020.1859161>

Publisher's Note Springer Nature remains neutral with regard to jurisdictional claims in published maps and institutional affiliations.